Dopant Concentration and Short-Range Structure Dependence of Diffusional Proton Dynamics in Hydrated BaIn x Zr 1– x O 3– x /2 (x = 0.10 and 0.50)

ARTICLE *in* THE JOURNAL OF PHYSICAL CHEMISTRY C · FEBRUARY 2010

Impact Factor: 4.77 · DOI: 10.1021/jp910224s

4 AUTHORS, INCLUDING:

Maths Karlsson
Chalmers University of Technology
40 PUBLICATIONS **350** CITATIONS
SEE PROFILE

Peter Fouquet
Institut Laue-Langevin
82 PUBLICATIONS **1,050** CITATIONS
SEE PROFILE

Istaq Ahmed
Chalmers University of Technology
23 PUBLICATIONS **369** CITATIONS
SEE PROFILE

Dopant Concentration and Short-Range Structure Dependence of Diffusional Proton Dynamics in Hydrated $BaIn_xZr_{1-x}O_{3-x/2}$ ($x = 0.10$ and 0.50)

Maths Karlsson,*,† Peter Fouquet,‡ Istaq Ahmed,§ and Marco Maccarini‡

European Spallation Source Scandinavia, Lund University, SE-221 00 Lund, Sweden, Institut Laue-Langevin, 6 rue Jules Horowitz, BP 156, 38042, Grenoble Cedex 9, France, and Department of Chemical and Biological Engineering, Chalmers University of Technology, SE-412 96 Göteborg, Sweden

Received: October 26, 2009; Revised Manuscript Received: January 14, 2010

We investigate proton self-dynamics in the acceptor-doped and hydrated proton-conducting perovskite-type oxides $BaIn_xZr_{1-x}O_{3-x/2}$ ($x = 0.10$ and 0.50) on a microscopic length scale for temperatures in the range 470−525 K, using neutron spin−echo spectroscopy. For the highly doped material ($x = 0.50$), we observe a wide range of translational diffusional rates of the protons in the structure, on the nanosecond time scale and with an effective activation energy of about 0.75 eV. The wide distribution of diffusional rates is related to the In-doping, which creates local structural distortions of the average cubic structure and thus many structurally different configurations of the protons, each with slightly different energy barriers for the protonic motion. For the weakly doped material ($x = 0.10$), which has a more ordered local structure, the results show proton dynamics on a much more well-defined time scale, ∼60 ps at 500 K, but also suggest that a significant part of the protons in the structure are "immobile" within the experimental neutron spin−echo time window (∼5 ps to 1.3 ns). Furthermore, the results indicate that the dopant atoms affect the proton diffusion in a nonlocalized manner and not as well-localized trapping centers.

1. Introduction

A number of ABO_3-type perovskites, e.g., $BaCeO_3$, $BaZrO_3$, and $SrZrO_3$, exhibit high proton conductivities in the intermediate temperature range (200−500 °C) after doping with trivalent acceptor-dopants and exposure to humid conditions, and thus are promising candidates to be used as electrolytes in future intermediate temperature fuel cells.[1] The acceptor-doping, such as In substituted for Zr in $BaZrO_3$, creates an oxygen-deficient structure, which under humid conditions absorbs water dissociatively so that the oxygen vacancies become filled with hydroxyl groups while the remaining protons bind to lattice oxygens. The protons are not stuck to any particular oxygens but move rather freely from one oxygen to another. It is generally believed that, on a local scale, the proton jumps between neighboring oxygens, residing on their crystallographic sites at intermediate temperatures, and performs a rotational motion around the oxygen to which it is covalently bound in between such transfers.[1] The long-range proton motion is thus supposed to be a series of the two elementary processes, with an overall rate that depends on the local energy barriers.

On microscopic length scales, proton dynamics in hydrated perovskites have been investigated with quasielastic neutron scattering (QENS), covering the picosecond time scale, extended up to ∼1 ns in some cases, in which mainly the local dynamical processes have been observed, although data have also been interpreted in terms of nonlocalized motions.[2−9] A particularly powerful method is neutron spin−echo (NSE),[10−12] which is the only QENS technique that covers a large time range of several decades, $\sim 10^{-12}-10^{-6}$ s, thus often enabling simultaneous investigations of dynamical processes on different time scales. Nevertheless, it was not until recently that the applicability of NSE spectroscopy for studies of proton diffusion in hydrated perovskites was demonstrated.[13] In that experiment, which was performed on 10% Y-doped and hydrated $BaZrO_3$, it was found that the protonic self-diffusion constant, measured over a length scale of 5−8 unit cell lengths, compared well to diffusion constants obtained from another neutron scattering technique[8] and from conductivity measurements[14] of the same material.

In this paper we investigate proton self-dynamics in the proton-conducting hydrated perovskites $BaIn_xZr_{1-x}O_{3-x/2}$ ($x = 0.10$ and 0.50), using NSE spectroscopy. The investigated materials exhibit an average cubic structure (space group $Pm\bar{3}m$), with the dopant (In) atoms randomly distributed over the Zr site,[15] but the In-doping develops short-range (local) structural distortions of the average cubic structure.[16] The structural distortions become more and more pronounced with increasing dopant level, and it has been suggested that the local structural distortions are related to tilting of the $(In/Zr)O_6$ octahedra due to the size difference between the In^{3+} and Zr^{4+} ions, and that there is a compositional "threshold" between $x = 0.10$ and 0.25 above which the dopant-induced structural distortions distribute throughout the entire perovskite structure.[16] Therefore, the choice of materials enables an investigation of how the proton dynamics depend on the local structure around the proton with the average cubic structure preserved. Such knowledge is of crucial importance for further development of these materials.

2. Experimental Methods

A. Sample Preparation. The $BaIn_xZr_{1-x}O_{3-x/2}$ ($x = 0.10$ and 0.50) powder samples were prepared through traditional solid state sintering by mixing appropriate amounts of $BaCO_3$, In_2O_3, and ZrO_2. The oxides were heated to 800 °C overnight to remove moisture prior to weighing. Milling was performed manually with use of an agate mortar and a pestle. The finely ground

* To whom correspondence should be addressed. E-mail: maths.karlsson@esss.se.
† Lund University.
‡ Institut Laue-Langevin.
§ Chalmers University of Technology.

10.1021/jp910224s
Published on Web 02/03/2010

mixtures were fired at 1000 °C for 8 h and subsequently ground and pelletized with a 13 mm diameter die under a load of 8 tons. The pellets were sintered at 1200 °C in air for 72 h. After sintering, the pellets were reground, compacted, and refired at 1500 °C for 48 h. Finally, the pellets were finely reground to powders. Charging with protons was performed by annealing the samples at ∼300 °C under a flow (12 mL/min) of N_2 saturated with water vapor at 76 °C over a period of 10 days. Thermal gravimetric analyses of In-doped $BaZrO_3$ show hydration levels in the range ∼60−90%,[14,15] and data from inelastic neutron scattering suggests that the degree of hydration is largely independent of the In concentration.[17] More specifically, the hydration levels have been determined from the change in mass of the sample during the hydration procedure and can be referred to as the percentage of filled oxygen vacancies. The hydrated $BaIn_xZr_{1-x}O_{3-x/2}$ (x = 0.10 and 0.50) samples are hereafter denoted as 10In:BZO and 50In:BZO, respectively.

X-ray diffraction measurements, carried out at ambient temperature on a Bruker AXS D8 ADVANCE VARIO powder diffractometer ($CuK\alpha_1$ = 1.54058 Å), confirmed an average cubic structure of space group $Pm\bar{3}m$ of both hydrated materials with unit cell parameters 4.193(4) Å (10In:BZO) and 4.2376(4) Å (50In:BZO), respectively.

B. Neutron Spin−Echo Experiment. The NSE experiment was performed at the IN11 spectrometer at Institut Laue-Langevin (ILL) in Grenoble, France. The spectrometer was set up using an incident wavelength of 5.5 Å and with the 30° wide-angle detector (option IN11C) centered at 55°, giving access to a dynamical range of ∼5 ps to 1.3 ns at the momentum transfers (Q) 0.83, 0.94, 1.05, 1.15, and 1.26 $Å^{-1}$. Spectra were measured at 1.5 and 500 K for 10In:BZO, and at 1.5, 470, 500, and 525 K for 50In:BZO. The 1.5 K spectra were measured for ∼30 h, while the spectra obtained at higher temperatures were measured for about half that time. The spectra measured at 1.5 K were used as resolution functions in the data analysis, since at this low temperature all diffusional motions of the protons are *frozen-in*, and the scattering of both samples is purely elastic in the NSE time window. The samples were loaded in Al containers and were 3 mm thick, which yielded a total scattering of neutrons of less than 10%, so that multiple scattering is negligible. It should be noted that for 10In:BZO, we only obtained data at the Q-values 0.94, 1.05, and 1.15 $Å^{-1}$ with satisfactory accuracy as a result of weak scattering due to this sample's relatively low proton concentration. To increase the statistics, we therefore summed the spectra obtained at the three different Q-values. The presented spectrum of 10In:BZO hence corresponds to an "average" Q-value of 1.05 $Å^{-1}$. The data analysis was performed with the standard IN11 data analysis package and FRIDA.[18]

3. Theoretical Background

In NSE spectroscopy one obtains the real part of the intermediate scattering function, $I(Q,t)$, which mathematically is the space Fourier transform of the space-time correlation function.[10−12] The normalized intermediate scattering function can be written as

$$\frac{I(Q,t)}{I(Q,0)} = \frac{\int S(Q,\omega)\cos(\omega t)\,d\omega}{\int S(Q,\omega)\,d\omega} \qquad (1)$$

where $S(Q,\omega)$ is the dynamic structure factor, which gives the probability that an incident neutron is scattered by the sample with a momentum transfer Q and energy transfer ω. $I(Q,t)/I(Q,0)$ is thus characterized by a decay with time related to the atomistic dynamics as resolved in the measurement. Furthermore, $I(Q,t)/I(Q,0)$ can be divided into a coherent and an incoherent part, which are related to the space Fourier transform of the space-time self- and pair-correlation functions, respectively, hence revealing the collective and self-dynamics simultaneously.[12]

In our case, we note that oxygen diffusion is negligible within the experimental NSE time window of ∼5 ps to 1.3 ns at the investigated temperatures.[14] Any decay of $I(Q,t)/I(Q,0)$ can therefore safely be related to proton dynamics. Moreover, we note that the incoherent neutron scattering cross section of protons is 80.3 barns, which is by far larger than the coherent one of 1.8 barns,[19] implying that largely self-dynamics is measured.

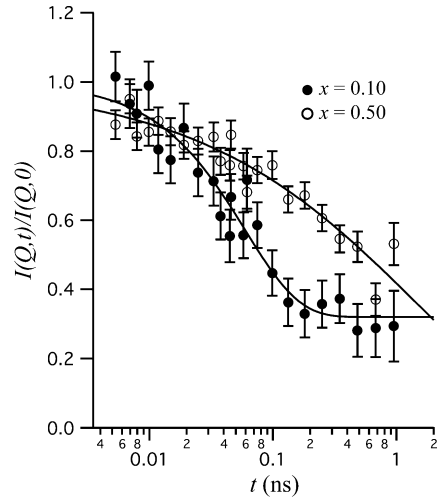

Figure 1. $I(Q,t)/I(Q,0)$ of 10In:BZO and 50In:BZO at 500 K and Q = 1.05 $Å^{-1}$. The lines represent fits with a single exponential function plus a constant (10In:BZO) and a KWW stretched exponential function (50In:BZO), respectively.

4. Results and Discussion

Figure 1 shows $I(Q,t)/I(Q,0)$ for 10In:BZO and 50In:BZO at 500 K and Q = 1.05 $Å^{-1}$. For both materials, we observe that $I(Q,t)/I(Q,0)$ is characterized by a relaxational decay in the experimental NSE time window ∼5 ps to 1.3 ns. It is also clear that the shape of the relaxational decay is significantly different for the two materials.

For the weakly doped material, 10In:BZO, we can describe the NSE data with a single exponential function of the form

$$\frac{I(Q,t)}{I(Q,0)} = [1 - c(Q)]e^{-t/\tau(Q)} + c(Q) \qquad (2)$$

where τ = 60 ps is a characteristic relaxation time of the relaxational process and c = 0.32. Here, the decay to a value larger than zero suggests that some of the protons in the structure are immobile on the probed time scale, since for the investigated Q-range of 0.83−1.26 $Å^{-1}$ contributions from coherent small-angle scattering and Bragg scattering are negligible and nearly all incoherent scattering can be associated to hydrogen. The data can equally well be described with a double exponential function of the form $I(Q,t)/I(Q,0) = [1 - A(Q)]\exp[-t/\tau_1(Q)] + A(Q)\exp[-t/\tau_2(Q)]$, where τ_1 = 55 ± 10 ns, τ_2 = 3.8 ± 6.5 ps, and A = 0.36 ± 0.07. Both fits are thus manifested by a fast relaxational process on largely the same time scale, 55−60 ps,

and with almost the same weight, 0.64−0.68, while the constant value in the single exponential fit is reflected by the second exponential in the double exponential fit. However, the double exponential fit does not add any additional information with reasonable accuracy since the error of τ_2 is very large. Hence, the use of a double exponential fit is not justified.

Previous investigations of proton dynamics in hydrated perovskites by QENS[2−9,13] and molecular dynamics (MD) simulations[20−23] have revealed local processes, notably interpreted as proton transfer between neighboring oxygens and rotational motion of the −OH group, on the time scale of picoseconds, whereas the translational proton diffusion is found to be a process on the nanosecond time scale. On these grounds we attribute the decay of $I(Q,t)/I(Q,0)$, which occurs on the picosecond time scale, to a local process. To determine the spatial geometry of this process is, however, not possible as we did not obtain the Q-dependence of the relaxation time.

In contrast to 10In:BZO, the data for 50In:BZO cannot be described by a simple exponential decay because the relaxation process is much more stretched in time. Instead, the data can be fitted to a Kohlrausch−Williams−Watts (KWW) stretched exponential function[24,25] according to

$$\frac{I(Q,t)}{I(Q,0)} = e^{-[t/\tau_{KWW}(Q)]^{\beta(Q)}} \quad 0 \le \beta \le 1 \qquad (3)$$

where $\tau_{KWW}(Q)$ is a characteristic time of a relaxational process and $\beta(Q)$ is the, so-called, stretching parameter. Figure 2 shows a good agreement for all Q-values and temperatures. However, also for this material, the spectra can be well described by a double exponential function. The reason why we have chosen to describe the data with a KWW stretched exponential is that the double exponential function requires one more fitting parameter and that the Q-dependence of one of the exponential functions in the double exponential fit is not systematic or, to our knowledge, in agreement with any model for diffusional dynamics. It is a more likely scenario that the protons have many different diffusional rates as a consequence of many local environments and that the KWW function therefore is a more relevant physical description of the data.

The idea of many different structural configurations of the protons in the perovskite structure is supported by results obtained from vibrational spectroscopy of the $BaIn_xZr_{1-x}O_{3-x/2}$ ($x = 0 - 0.75$) system,[16] showing that 50In:BZO exhibits pronounced short-range structural distortions of the average cubic structure. The structural distortions are related to tilting of the $(In/Zr)O_6$ units and are more pronounced for higher dopant levels.[16] Moreover, it has been suggested that there is a compositional "threshold", between $x = 0.10$ and 0.25, above which the dopant-induced structural distortions distribute throughout the crystallites.[16] This is indeed in agreement with our findings that for 10In:BZO the observed protonic self-dynamics have, in contrast to 50In:BZO, a much more well-defined time scale. The NSE results are also in agreement with recent data obtained from infrared (IR) spectroscopy.[26] For 50In:BZO, the IR spectrum is manifested by a broad O−H stretch band between 1700 and 3700 cm^{-1} while for 10In:BZO it is a more narrow band in the range 2500−3700 cm^{-1}.[26] The much broader nature of the O−H stretch band for 50In:BZO suggests a wider distribution of degree of hydrogen bonding between the protons and neighboring oxygens, O−H···O, as a result of many local environments of the protons in the structure, while the more narrow O−H stretch band for 10In:BZO suggests a less wide distribution of degree of hydrogen bonding, due to its more ordered local structure.[26]

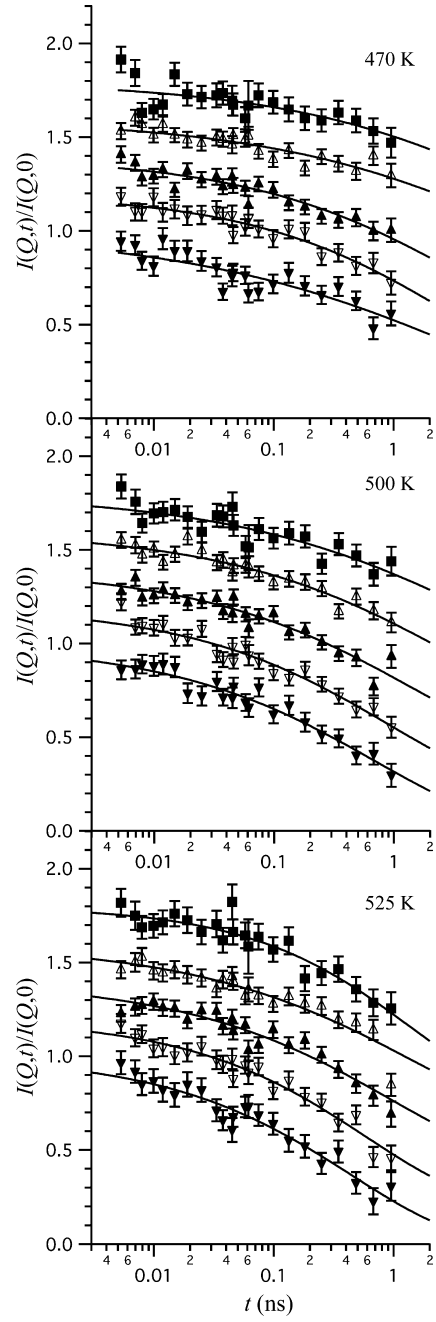

Figure 2. NSE spectra of 50In:BZO at 470, 500, and 525 K, and Q = 0.83, 0.94, 1.05, 1.15, and 1.26 $Å^{-1}$, where the solid lines are KWW fits according to eq 3. For clarity, the spectra are vertically separated by 0.2, with the lowest Q-value uppermost.

Figure 3 shows the Q-dependence of the stretching parameter, β, for the three different temperatures, and as seen, β is basically independent of Q within the statistical uncertainty. The Q-independence of β within the measured Q-range 0.83−1.26 $Å^{-1}$, corresponding to length scales between 5 and 7.6 Å in real space,[27] is consistent with the suggestion that the structural distortions are extended throughout the entire perovskite lattice, since it implies that the neutrons will "see" the same, or at least similar, magnitude of structural distortions regardless of the probed Q-value. At smaller Q-values, corresponding to longer distances in real space, than those probed in the present NSE experiment, the wide distribution of diffusional rates would tend

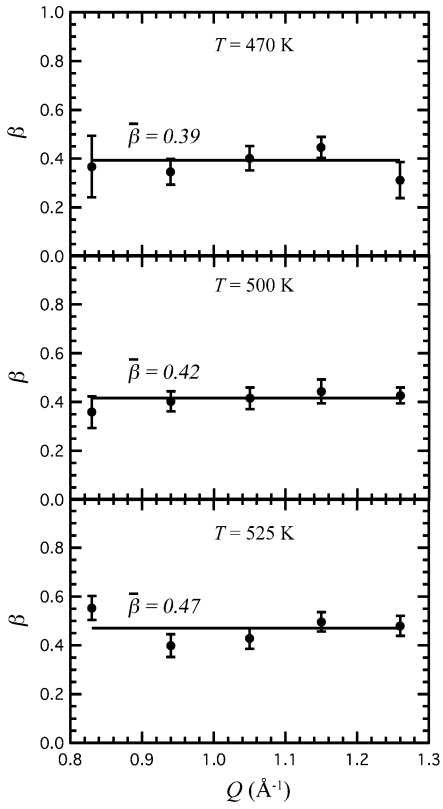

Figure 3. Q-dependence of the stretching parameter, β. The linear lines are least-squares fits, which give the Q-averaged values of β.

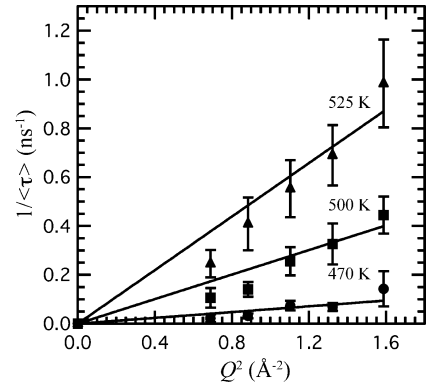

Figure 4. Inverse of the average relaxation time as a function of Q^2. The solid lines are linear fits whose slopes are the effective self-diffusion constant, D. The fits have been forced to go through origo.

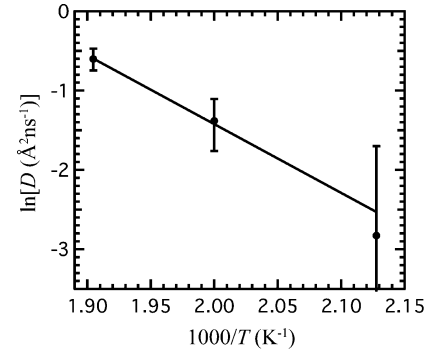

Figure 5. Arrhenius graph of the effective self-diffusion constant D. The linear fit corresponds to an activation energy $E_a = 0.75 \pm 0.23$ eV.

to average out and one would hence expect a less stretched form of the decay of $I(Q,t)$, and ultimately a single exponential as $Q \rightarrow 0$.

The lines in Figure 3 are linear fits of the data to obtain a mean value of the stretching parameter ($\bar{\beta}$) for each temperature and we find that $\bar{\beta}$ increases gradually with temperature, from 0.39 at 470 K up to 0.47 at 525 K. This suggests that the distribution of diffusional rates becomes more narrow as the temperature increases, likely as an effect of the protons having sufficient energy to surpass their local energy barriers. This is consistent with temperature-dependent IR spectra of 50In:BZO, which show a pronounced suppression of the low-frequency part of the O−H stretch band with increasing temperature, suggesting that the distribution of the degree of hydrogen bonding narrows.[26]

The obtained $\bar{\beta}$-values have been used to calculate the average relaxation times $\langle\tau(Q)\rangle$ for each temperature by the relation

$$\langle\tau(Q)\rangle = \frac{\tau(Q)}{\bar{\beta}}\Gamma[1/\bar{\beta}(Q)] \qquad (4)$$

where Γ is the Gamma function.[24,25] The Q-dependence of $\langle\tau(Q)\rangle$ provides information about the physical properties of the proton self-dynamics. For example, for free translational self-diffusion we have $1/\tau(Q) = DQ^2$, where D is the self-diffusion constant. In fact, this relationship holds well for our data as shown in Figure 4, and we have therefore extracted a diffusion constant at each temperature. At 525 K the protonic self-diffusion constant is 5.5×10^{-8} cm^2 s^{-1}, which is in the same range as those values obtained from conductivity measurements of In-doped $BaZrO_3$ (1.3×10^{-8} cm^2 s^{-1} for 10In:BZO,[14] and 2.8×10^{-8} cm^2 s^{-1} for 75In:BZO,[15] at 573 K). One should note, however, that the self-diffusion constant obtained from the NSE data is not the true long-range proton self-diffusion constant but rather an effective self-diffusion constant reflecting a distribution of more local diffusional rates.

Figure 5 displays the effective self-diffusion constant, D, obtained from the NSE data in an Arrhenius plot, from which we have extracted the activation energy for the protonic self-diffusion from a linear fit. The activation energy is found to be $E_a = 0.75 \pm 0.23$ eV. This can be compared to previous investigations of proton dynamics in hydrated perovskites, which have mostly revealed activation energies for translational proton diffusion in the range 0.4−0.6 eV.[14]

In this context, we note that there are two different views on how the dopant atoms affect the proton diffusivity in acceptor-doped and hydrated perovskites. Several researchers claim that the dopant atoms act as well-localized trapping centers, where the proton spends an extended period of time before it diffuses further throughout the structure. This view was first introduced on the basis of QENS data of $SrCe_{0.95}Yb_{0.05}H_{0.02}O_{2.985}$, which could be fitted to a, so-called, two-state model, suggesting that the proton migration takes place through a sequence of trapping and release events.[2] This view has been supported by muon spin-relaxation measurements,[28] and computer simulations.[29−31] Converse to this picture, it has been proposed that the dopant atoms affect the proton transport in a more nonlocal fashion.[32,33] This suggestion was based on conductivity data of Y-doped and hydrated $BaCeO_3$, which showed that the proton conductivity decreased with increasing dopant level.[32,33] This decrease was, however, not a result of a decrease of the pre-exponential factor, D_0, in the expression for the diffusivity, $D = D_0 \exp(-E_a/k_BT)$, as anticipated by the two-state model, but instead mainly a result of an increased activation energy, E_a. The fact that the activation energy for 50In:BZO as extracted from the NSE data is relatively

large compared to those typical values found in the literature for hydrated perovskites, and that the dopant level is high ($x = 0.50$), would thus give preference for such a nonlocalized picture of the effect of dopant atoms on the protonic motions. However, it should be noted that from the present experiment we did not obtain the activation energy for $x = 0.10$ for comparison, and more investigations are needed to clarify if the effect is the same for different dopant atoms.

5. Conclusions

By using neutron spin−echo spectroscopy we have investigated proton self-dynamics in the proton-conducting hydrated perovskites $BaIn_xZr_{1-x}O_{3-x/2}$ ($x = 0.10$ and 0.50) in the picosecond to nanosecond time range for different momentum transfers ($Q = 0.83-1.26$ Å^{-1}) and temperatures (470−525 K). The results show that the proton self-dynamics are highly dependent on the In concentration and the short-range structure of the material. For the highly doped material ($x = 0.50$), we observe a distribution of translational diffusional rates of the protons in the structure on the time scale of nanoseconds and with an effective activation energy of about 0.75 eV. The wide range of diffusional rates is related to the In-doping, which creates local structural distortions of the average cubic structure and, concomitantly, many structurally different configurations of the protons, each with slightly different energy barriers for the protonic motion. For comparison, the data of the weakly doped compound ($x = 0.10$) reveal dynamics on more well-defined time scales as a result of a more ordered local structure. Moreover, the results indicate that the dopant atoms affect the proton self-diffusion in a quite nonlocalized manner and not as well-localized trapping centers as frequently suggested in the literature.

Acknowledgment. Financial support by the Swedish Research Council and allocation of beam time at ILL is gratefully acknowledged. We are grateful for technical assistance by E. Thaveron, technician at the IN11 spectrometer, and to M. Björketun at Technical University of Denmark for fruitful discussions.

References and Notes

(1) Kreuer, K. D. *Annu. Rev. Mater. Res.* **2003**, *33*, 333.
(2) Hempelmann, R.; Karmonik, C.; Matzke, T.; Cappadonia, M.; Stimming, U.; Springer, T.; Adams, M. A. *Solid State Ionics* **1995**, *77*, 152.
(3) Matzke, T.; Stimming, U.; Karmonik, C.; Soetramo, M.; Hempelmann, R.; Güthoff, F. *Solid State Ionics* **1996**, *86−88*, 621.
(4) Gross, B.; Beck, C.; Meyer, F.; Krajewski, T.; Hempelmann, R.; Altgeld, H. *Solid State Ionics* **2001**, *145*, 325.
(5) Karlsson, M.; Matic, A.; Engberg, D.; Björketun, M. E.; Koza, M. M.; Ahmed, I.; Wahnström, G.; Berastegui, P.; Börjesson, L.; Eriksson, S. G. *Solid State Ionics* **2009**, *180*, 22.
(6) Karmonik, C.; Hempelmann, R.; Cook, J.; Güthoff, F. *Ionics* **1996**, *2*, 69.
(7) Pionke, M.; Mono, T.; Schweika, W.; Springer, T.; Schober, H. *Solid State Ionics* **1997**, *97*, 497.
(8) Wilmer, D.; Seydel, T.; Kreuer, K. D. *Mater. Res. Soc. Symp. Proc.* **2007**, *15*, 972.
(9) Braun, A.; Duval, S.; Ried, P.; Embs, J.; Juranyi, F.; Strässle, T.; Stimming, U.; Hempelmann, R.; Holtappels, P.; Graule, T. *J. Appl. Electrochem.* **2009**, *39*, 262103.
(10) Mezei, F. *Neutron Spin Echo: Lecture Notes in Physics*; Springer: Heidelberg, Germany, 1980; Vol. 28.
(11) Mezei, F. *Z. Phys.* **1972**, *255*, 146.
(12) Mezei, F.; Pappas, C.; Gutberlet, T. *Neutron Spin Echo Spectroscopy; Basics, Trends and Applications*; Springer: New York, 2003.
(13) Karlsson, M.; Engberg, D.; Björketun, M. E.; Matic, A.; Wahnström, G.; Sundell, P. G.; Berastegui, P.; Ahmed, I.; Falus, P.; Farago, B.; Börjesson, L.; Eriksson, S. *Chem. Mater.* **2009** In press.
(14) Kreuer, K. D.; Adams, S.; Münch, W.; Fuchs, A.; Klock, U.; Maier, J. *Solid State Ionics* **2001**, *145*, 295.
(15) Ahmed, I.; Eriksson, S. G.; Ahlberg, E.; Knee, C. S.; Berastegui, P.; Johansson, L. G.; Rundlöf, H.; Karlsson, M.; Matic, A.; Börjesson, L.; Engberg, D. *Solid State Ionics* **2006**, *177*, 1395.
(16) Karlsson, M.; Matic, A.; Knee, C. S.; Ahmed, I.; Börjesson, L.; Eriksson, S. G. *Chem. Mater.* **2008**, *20*, 3480.
(17) Karlsson, M.; Matic, A.; Parker, S. F.; Ahmed, I.; Börjesson, L.; Eriksson, S. G. *Phys. Rev. B* **2008**, *77*, 104302.
(18) http://sourceforge.net/projects/frida (accessed Oct. 23, 2009).
(19) http://www.ncnr.nist.gov/resources/n-lengths (accessed Oct. 23, 2009).
(20) Münch, W.; Seifert, G.; Kreuer, K. D.; Maier, J. *Solid State Ionics* **1996**, *86−88*, 647.
(21) Münch, W.; Seifert, G.; Kreuer, K. D.; Maier, J. *Solid State Ionics* **1997**, *97*, 39.
(22) Kreuer, K. D.; Münch, W.; Traub, U.; Maier, J. *Ber. Bunsenges. Phys. Chem.* **1998**, *102*, 552.
(23) Shimojo, F.; Hoshino, K.; Okazaki, H. *J. Phys. Soc. Jpn.* **1997**, *66*, 8.
(24) Kohlrausch, R. *Ann. Phys. (Weinheim, Ger.)* **1854**, *1*, 179.
(25) Williams, G.; Watts, D. C. *Trans. Faraday Soc.* **1970**, *66*, 80.
(26) Karlsson, M.; Matic, A.; Zanghellini, E.; Ahmed, I. Submitted for publication.
(27) The estimation of the length scale in real space (d) is determined from the momentum transfer (Q) through $d = 2\pi/Q$, a relationship that is often used in the literature.
(28) Hempelmann, R.; Soetramo, M.; Hartmann, O.; Wäppling, R. *Solid State Ionics* **1998**, *107*, 269.
(29) Islam, M. S.; Davies, R. A.; Gale, J. D. *Chem. Mater.* **2001**, *13*, 2049.
(30) Davies, R. A.; Islam, M. S.; Gale, G. D. *Solid State Ionics* **1999**, *126*, 323.
(31) Islam, M. S.; Slater, P. R.; Tolchard, J. R.; Dinges, T. *Dalton Trans.* **2004**, 3061–3066.
(32) Kreuer, K. D. *Solid State Ionics* **1999**, *125*, 285.
(33) Kreuer, K. D. *Solid State Ionics* **1997**, *97*, 1.

JP910224S